Direct photoeffect in heavy deformed nuclei at $E_\gamma \lesssim 40$ MeV

V. N. Orlin and K. A. Stopani*
Lomonosov Moscow State University, Skobeltsyn Institute of Nuclear Physics, Moscow 119991, Russia

(Received 27 April 2023; revised 14 October 2023; accepted 24 October 2023; published 20 November 2023)

The mechanism of direct knockout of a nucleon from heavy deformed nuclei with $A \gtrsim 100$ by photons in the $E_\gamma \lesssim 40$ MeV energy range is considered, and the interaction of the ejected nucleon with the rotational degrees of freedom of the final nucleus is taken into account. It is assumed that the rotation frequency of the nucleus is much less than the frequency of its surface vibrations and the Siegert's theorem is in effect. This model was applied to calculation of the total and differential cross sections of direct proton knockout reactions on ^{108}Pd, ^{160}Gd, and ^{184,186}W and the bremsstrahlung-induced yield of photoprotons on ^{180}Hf. Comparison with the experimental data and with the results of a statistical model calculation indicates importance of the direct photoeffect for such nuclei in the considered energy range. Calculations show that for deformed nuclei the interaction of the ejected nucleon with the rotational excitations of the final nucleus results in a significant enhancement of the direct photoeffect cross section. Angular distribution of ejected protons reveals a large asymmetry in the forward direction at $E_\gamma > 20$ MeV.

DOI: 10.1103/PhysRevC.108.054606

I. INTRODUCTION

The direct nucleon knockout mechanism (DKO) of nuclear photoeffect is an ejection of one of the bound nucleons into a continuum state by the absorbed photon while the final nucleus stays in a certain nucleon hole state. It is assumed that the initial and final nuclear states can be described in terms of the independent-particle shell model, and the motion of the ejected nucleon takes place in the potential that is a result of averaging of its interaction with the remaining nucleons.

The mechanism of the direct knockout of a single proton by a real photon (proton DKO) has been extensively discussed during the last decades [1–17]. In a number of nonrelativistic calculations [2,6,8–10,13,16] it was shown that the proton DKO contribution at intermediate photon energies of about $E_\gamma \approx 60$ MeV may be much smaller than the experimental photoproton yield and, in order to explain the observed cross sections, one has to take into account the fact that meson exchange currents can lead to photoabsorption by pairs of strongly correlated nucleons of which only one is emitted and the other is reabsorbed in the residual nucleus. These conclusions are significantly different from what follows from the results of the relativistic calculations of Johannson *et al.* [11], who showed that for a 60 MeV incident photon the contribution of DKO comprises the greater part of the observed data. Subsequent studies [12] in this direction performed for a larger number of nuclei and incident energies have confirmed that in relativistic calculations the direct contribution is, on the whole, close to the experimental data when the transferred momentum is less than 500 MeV/c. This suggests that within the relativistic approach the contribution of the meson exchange currents is not as large. This conclusion is further confirmed by the relativistic DKO calculations of the cross section for the ^{16}O$(\gamma, p)^{15}$N reaction, performed in Ref. [17] at $E_\gamma \approx 60$–200 MeV where, however, it is noted that consideration of the meson exchange currents noticeably improves agreement with the experiment.

It should be mentioned that the DKO model has been mainly applied to relatively light closed-shell nuclei (most often to ^{12}C, ^{16}O, and ^{40}Ca), and for this the spectroscopic factors obtained from the analysis of the quasifree electron scattering process $(e, e'p)$ were used. At the same time, for heavy deformed nuclei one has to take into account the possibility that knockout of a surface nucleon—a process playing an important role at a relatively moderate transferred momentum—results in excitation of low-lying collective rotational states of the final nucleus belonging to the rotational band built upon the produced nucleon hole. Each of such states forms a separate exit channel of the reaction, but there exists a strong connection among them in the internal region of the reaction, because deformation of a nonspherical nucleus leads to interaction between the rotational degrees of freedom of the final nucleus and the orbital motion of the outgoing particle. Application of the DKO model in this case will require solution of the system of equations of the coupled reaction channels method.

In the present work a model of direct nucleon knockout from heavy deformed nuclei at comparatively small energies of the absorbed photon $E_\gamma \lesssim 40$ MeV is developed. The interest to such calculations is inspired by the fact that statistical reaction models based on the Bohr's compound nucleus hypothesis frequently give an apparently underestimated, in comparison with the experimental data, value of the (γ, p) reaction cross section on heavy deformed nuclei at E_γ 25–30 MeV, which, at least in some cases, is a result of the neglect of the contribution of the direct photoeffect to this cross section.

In the considered case, the knockout of the nucleon takes place mostly at the nuclear surface, where the nucleon density is lower, and, as a result, the nucleon with a large probability

*Corresponding author: kstopani@sinp.msu.ru

is knocked out into the continuum. This allows us to limit ourselves to consideration of the knockout of bound nucleons only from the single-particle levels of the target nucleus A near the Fermi surface. At $E_\gamma \lesssim 40$ MeV the direct photoeffect proceeds mostly due to $E1$ and $E2$ electric transitions, and while the $E2$ transitions do not contribute much to the total cross section of the direct photonucleon knockout, but their interference with the $E1$ transitions results in a large asymmetry of the ejected nucleons in the forward direction. The computational complexity of the DKO model is significantly simplified if one uses the Siegert's theorem for calculation of the matrix elements of $E1$ and $E2$ transitions since it allows to use the nonrelativistic form of DKO without explicit consideration of the meson exchange currents. According to the Siegert's theorem the current density operator in the matrix elements of electric transitions can be substituted with the charge density operator, for which, in the case of a multipole transition L, in the first approximation, it is sufficient (see, e.g., [18]) that $\delta_L(kR) \equiv [j_{L+1}(kR)/j_{L-1}(kR)]\sqrt{L/(L+1)} \ll 1$, where $j_L(x)$ is the spherical Bessel function, $k = E_\gamma/c\hbar$ fm^{-1} is the wave vector transferred to the nucleus, and $R \approx 1.2A^{1/3}$ fm is the nuclear radius. This condition is, clearly, satisfied for heavy nuclei with $A \lesssim 200$ in the considered energy range: for a nucleus with $A = 160$, the parameter $\delta_1(kR)$ corresponding to $E1$ transitions at $E_\gamma = 30$ MeV is equal to 0.05, and the parameter $\delta_2(kR)$ is about twice as small.

This work presents a continuation of the formalism developed in Ref. [19], where a straightforward version of the DKO model of the direct nuclear photoeffect was implemented, but the interaction of the knocked out nucleon with the rotational degrees of freedom of the final nucleus was not taken into consideration. As it will be shown its contribution has a significant effect on the resulting reaction cross section.

The developed model is described in Secs. II–V. In Sec. VI the constructed model is applied to proton DKO in ^{108}Pd, ^{160}Gd, ^{184,186}W, and ^{180}Hf. Section VII contains a discussion of the obtained results.

II. MAIN STATEMENTS OF THE MODEL

(1) It is assumed in the standard formulation of the DKO mechanism (see, e.g., Ref. [4]) that the absorbed photon knocks out a single bound nucleon, transferring it to a continuum state, while the final nucleus remains in a certain nucleon hole state. It is expected that both the initial and final nuclear states can be described in terms of the independent-particle shell model. Thus, the knocked out nucleon performs an electromagnetic transition between a bound and a continuous single-particle state of the average potential, which is produced by the rest of the nucleons and is fixed with respect to the laboratory frame.

Such description seems appropriate for spherical nuclei with closed shells. However, as the number of particles above the closed shells increases the situation becomes more complicated, and one can not rely on simple single-particle shell-model calculations for description of the direct nuclear photoeffect.

The other limiting case, opposite to the case of closed-shell nuclei, is considered in this work, when usage of the DKO mechanism once again becomes practical for description of the direct nuclear photoeffect. Namely, this is the case of heavy deformed nuclei. Such nuclei as a rule have a nonspherical shape, stable with respect to surface oscillations, which allows one to consider a specific orientation of the nucleus in the surrounding space and to approximately separate motion of individual nucleons in the intrinsic coordinate frame of the nucleus from its collective rotational motion as a whole in the laboratory frame (strong coupling scheme). Such separation is possible if the system satisfies the adiabatic condition, that is, the frequency of the rotational motion of the nucleus has to be much less than the frequency of oscillations of its surface, which implies smallness of the amplitude of the surface oscillations compared to the size of the nucleus. In this case the wave function of the nucleus, representing a solution of the stationary Schrödinger equation in the laboratory frame, has the form of a product of two parts: one describing the rotation of the nucleus and another describing the intrinsic motion of nucleons in the fixed average field [20].

In the considered case the nucleon knocked out by a photon performs an electromagnetic transition from a bound internal single-particle state in the fixed average field produced by the rest of the nucleons to a continuous single-particle state in this field in the laboratory frame, and because in the laboratory frame the average field created by the nucleons of the final nucleus depends on its orientation in space, a connection between the orbital motion of the emitted nucleon and the rotational degrees of freedom of the final nucleus arises.

(2) Only axially symmetric deformed nuclei are considered. We will also assume that it is not necessary to take into account antisymmetrization of the knocked out (and, therefore, labeled) nucleon with the rest of the nucleons of the target nucleus, which allows us to express the ground state of the target nucleus $|J_0M_0\rangle$ in the laboratory frame with the z axis directed along the incident photon direction as a product

$$|J_0M_0\rangle = \left(\frac{2J_0+1}{8\pi^2}\right)^{1/2} D^{J_0}_{M_0\Omega+K}(\omega)\varphi'_{\beta\Omega}\chi'_{\beta K}, \quad (1)$$

where β is the index of the orbit from which the nucleon will be knocked out, $\varphi'_{\beta\Omega}$ is the wave function of the knocked out nucleon in the intrinsic frame, $\chi'_{\beta K}$ is the wave function describing the state of the remaining nucleons of the target nucleus in the intrinsic frame, Ω is the projection of the total angular momentum of the knocked out nucleon onto the nucleus's symmetry axis, K is the projection of the total angular momentum of the remaining nucleons onto the symmetry axis, $J_0 = |\Omega + K|$ is the magnitude of the total angular momentum $\mathbf{J}_0$ of the target nucleus in the laboratory

frame, M_0 is its z-axis projection in the laboratory frame, $\Omega + K$ is the projection of $\mathbf{J}_0$ on the symmetry axis, ω are the Euler rotation angles, describing the orientation of the intrinsic coordinate frame relative to the laboratory frame, $D^{J_0}_{M_0\Omega+K}(\omega)$ is the matrix of finite rotation from the laboratory frame to the intrinsic frame.

(3) It is assumed that at $E_\gamma \lesssim 40$ MeV the direct photoeffect in heavy deformed nuclei with $A \gtrsim 100$ proceeds mainly via direct knockout of nucleons from the filled single-particle states of the target nucleus A, positioned near the Fermi surface.

(4) It is assumed that when the nucleon is knocked out from a certain near-surface orbit β the intrinsic state of the rest of the nucleons $\chi'_{\beta K}$ stays unchanged (together with the average nuclear field produced by them), and, therefore, only the states $|n\rangle$ of the rotational band of the final nucleus, corresponding to the produced nucleon hole excitation of the target nucleus, can be excited:

$$|n\rangle = \left(\frac{2I_n+1}{8\pi^2}\right)^{1/2} D^{I_n}_{M_nK}(\omega)\chi'_{\beta K}, \tag{2}$$

where $n = 1, 2, \ldots, n_{\max}$, I_n is the magnitude of the angular momentum of the final nucleus, M_n and K are its projections onto the z axis of the laboratory frame and the nucleus's symmetry axis, respectively.

(5) The transition rate from the ground state of the target nucleus to the state describing the scattering of the knocked out photonucleon by the nucleons of the final nucleus is calculated within the time-dependent perturbation theory. The Siegert's theorem is used for calculation of the matrix elements of electric transitions.

III. EQUATIONS OF SCATTERING OF THE KNOCKED OUT NUCLEON

The Hamiltonian operator, describing scattering of the knocked out nucleon in the potential of the final nucleus in the laboratory frame can be written as

$$H = T + H_{fin} + V, \tag{3}$$

where

$$T = \frac{-\hbar^2\Delta_{\mathbf{r}}}{2\mathcal{M}}, \tag{4}$$

is the kinetic energy operator of the knocked out nucleon ($\mathcal{M}$ is the nucleon mass),

$$H_{\text{fin}} = H_{\text{int}} + H_{\text{rot}}, \tag{5}$$

is the Hamiltonian of the final nucleus, which is comprised of two terms: H_{int} describing the internal state $\chi'_{\beta K}$ of the final nucleus [see (2)] and H_{rot}, its rotation. V is the complex potential describing the interaction of the outgoing nucleon with the final nucleus.

The potential V is comprised of the nuclear interaction term, the spin-orbit term, and, in the case of proton knockout, the Coulomb interaction term. During construction of the potential we neglect the effect of the nucleus's deformation on the spin-orbit interaction, similarly to Ref. [21], and define V as

$$V = V_{\text{so}} + V_{\text{coupl}}, \tag{6}$$

where the spherical potential V_{so} describes the spin-orbit interaction, while the V_{coupl} term is comprised of the remaining (nonspherical) components of the potential V.

The V_{so} potential is taken in the form of the spin-orbit part of the spherical global optical potential [22]. The nonspherical potential $V_{\text{coupl}}(r, \vartheta')$ is obtained (in the intrinsic reference frame) from the nuclear and Coulomb interaction terms of this optical potential using the deformation procedure described in Refs. [19,23], corresponding to an axially symmetric ellipsoidally deformed nucleus with the axial deformation parameter δ.

In order to find the potential V in the laboratory frame one has to expand the potential $V_{\text{coupl}}(r, \vartheta')$ in the intrinsic frame into spherical harmonics and transform the harmonics to the laboratory frame via rotation by the Euler angles ω. As a result one obtains:

$$V = V_{\text{so}} + \sum_{\lambda\nu} v_\lambda(r) D^{\lambda *}_{\nu 0}(\omega) Y_{\lambda\nu}(\vartheta, \varphi), \tag{7}$$

where λ takes only even values (since only spheroidal shapes are considered) and the coefficients of the expansion are determined by the expressions

$$v_\lambda(r) = \int V_{\text{coupl}}(r, \vartheta') Y^*_{\lambda 0}(\vartheta') d\Omega'. \tag{8}$$

Since the introduced spin-orbit interaction does not change under rotation of the coordinate axes, the coupling between different channels (l, j, n) arises only due to the deformed part of the potential V_{coupl}.

We will consider the knocked out nucleon state within the time-independent scattering theory. Solutions Ψ of the stationary Schrödinger equation corresponding to the Hamiltonian (3) can be divided into two groups: (i) bound states with a discrete spectrum, (ii) continuum states satisfying particular boundary conditions. We are interested in the continuum states satisfying the boundary condition

$$\Psi \to |\mathbf{k}s\rangle|n\rangle \equiv |\mathbf{k}s, n\rangle \quad \text{when } r \to \infty, \tag{9}$$

where $\langle \mathbf{r}\sigma|\mathbf{k}s\rangle = \frac{1}{(2\pi)^{3/2}} e^{i\mathbf{kr}} \chi_{\frac{1}{2}s}(\sigma)$ is the state of free motion of a nucleon with the wave vector $\mathbf{k}$ and z projection of the spin $s = \pm 1/2$, and $|n\rangle$ is the state of the final nucleus [see (2)], corresponding to the nth level of the considered rotational band.

It is known from the time-independent scattering theory (see Refs. [24–26]) that the eigenstates $|(\mathbf{k}s, n)^{(-)}\rangle$ of the H operator meeting the boundary condition (9) satisfy the integral Lippmann-Schwinger equation for converging-wave states:

$$|(\mathbf{k}s, n)^{(-)}\rangle = |\mathbf{k}s, n\rangle + \frac{1}{\varepsilon + E_n - H - i\rho} V |(\mathbf{k}s, n)^{(-)}\rangle, \tag{10}$$

where $\rho \to 0^+$, $\varepsilon = \frac{\hbar^2 k^2}{2M} = E_\gamma - B - E_n$ is the outgoing nucleon energy, B is the separation energy of the nucleon from

the target nucleus, $E_n = \varepsilon_F - \varepsilon_\beta + \frac{\hbar^2[I_n(I_n+1)-K(K+1)]}{2\mathcal{T}}$ is the excitation energy of the final nucleus, ε_F and ε_β are, respectively, the Fermi energy and the energy of the single-particle state $|\beta\rangle$ of the target nucleus, $\mathcal{T}$ is the moment of inertia of the final nucleus.

The $|(\mathbf{k}s, n)^{(-)}\rangle$ state is an eigenstate of H with the energy $\varepsilon + E_n$. The required boundary condition is provided by the "$-$" sign of ρ in (10). It can also be shown from Eq. (10) that these states satisfy the normalization conditions

$$\langle(\mathbf{k}'s', n')^{(-)}|(\mathbf{k}s, n)^{(-)}\rangle = \delta_{n'n}\delta_{s's}\delta(\mathbf{k}' - \mathbf{k}). \tag{11}$$

It should be noted that inside the interaction region the quantities $(\mathbf{k}, s, E_n, I_n, M_n)$, specifying the emitted nucleon and the final nucleus, are not conserved. They take definite values after the nucleon leaves the interaction region, i.e., at $r \to \infty$.

Using the expansion of the wave function $(2\pi)^{-3/2}e^{i\mathbf{kr}}$ of a free particle with a definite momentum $\hbar\mathbf{k}$ into wave functions $\psi_{\varepsilon lm}$ of free motion with a definite energy ε and orbital quantum numbers l, m [27] one can express the scattering state $|(\mathbf{k}s, n)^{(-)}\rangle$ in the form

$$|(\mathbf{k}s, n)^{(-)}\rangle = \frac{\hbar}{\sqrt{\mathcal{M}k}} \sum_{l=0}^{\infty} \sum_{j=|l-\frac{1}{2}|}^{l+\frac{1}{2}} \sum_{m=-j}^{j} \left(lm - s\,\frac{1}{2}s|jm\right) \times Y^*_{lm-s}(\theta, \phi)|(\alpha, n)^{(-)}\rangle, \tag{12}$$

where (θ, ϕ) are the polar and azimuthal angles of the direction of the outgoing nucleon in the laboratory frame, $|(\alpha, n)^{(-)}\rangle \equiv |(\varepsilon, l, j, m; n)^{(-)}\rangle$ is the eigenstate of the Hamiltonian H with the energy $\varepsilon + E_n$, which at $r \to \infty$ is asymptotically equal to the state $|\alpha, n\rangle$ describing the free motion of a nucleon with the energy ε, orbital momentum l, total angular momentum j, and its z projection m in the laboratory frame and the state of the final nucleus $|n\rangle$ belonging to the considered rotational band.

In the interaction region the state $|(\alpha, n)^{(-)}\rangle$ has a definite value of the energy $\varepsilon + E_n$, parity $\pi = (-1)^l\pi_n$, and z projection $m + M_n$ of the total angular momentum $\mathbf{J} = \mathbf{j} + \mathbf{I_n}$ in the laboratory frame. At the same time the quantum numbers $\varepsilon, l, j, m, E_n, I_n, M_n$ are not conserved inside this region due to the interaction of the knocked out nucleon with the nucleons of the final nucleus via the deformed average field. Note, however, that the parity of the final nucleus π_n is fixed, since knockout of the nucleon takes place from a particular orbit β of the target nucleus. Thus, at a given multipolarity of the photon, the parity of the outgoing nucleons has a definite value $(-1)^l$.

Later in the discussion we use the scattering state

$$|(\alpha, n)^{(-)}_{JM}\rangle = \sum_{mM_n}(jmI_nM_n|JM)|(\alpha, n)^{(-)}\rangle \tag{13}$$

having definite values of the total angular momentum J and its z-axis projection M.

The inverse transformation for (13) has the form

$$|(\alpha, n)^{(-)}\rangle = \sum_{JM}(jmI_nM_n|JM)|(\alpha, n)^{(-)}_{JM}\rangle. \tag{14}$$

It allows us to express the expansion (12) as

$$|(\mathbf{k}s, n)^{(-)}\rangle = \frac{\hbar}{\sqrt{\mathcal{M}k}} \sum_{ljmJM} \left(lm - s\,\frac{1}{2}s|jm\right) Y^*_{lm-s}(\theta, \phi) \times (jmI_nM_n|JM)|(\alpha, n)^{(-)}_{JM}\rangle. \tag{15}$$

The states $|(\alpha, n)^{(-)}_{JM}\rangle$ satisfy the equation

$$|(\alpha, n)^{(-)}_{JM}\rangle = |(\alpha, n)_{JM}\rangle + \frac{1}{\varepsilon + E_n - H_0 - i\rho}V|(\alpha, n)^{(-)}_{JM}\rangle, \tag{16}$$

where $|(\alpha, n)_{JM}\rangle \equiv |(\varepsilon, l, j; n)_{JM}\rangle$ is the state of the nuclear system with definite quantum numbers J and M, describing motion of a free nucleon with quantum numbers ε, l, j and the final nucleus in the given state $|n\rangle$ of the rotational band.

The normalization condition for the states $|(\alpha, n)^{(-)}_{JM}\rangle$ has the form

$$\langle(\alpha, n)^{(-)}_{JM}|(\alpha', n')^{(-)}_{J'M'}\rangle = \delta_{J'J}\delta_{M'M}\delta(\varepsilon' - \varepsilon)\delta_{l'l}\delta_{j'j}\delta_{n'n}. \tag{17}$$

IV. DIFFERENTIAL CROSS SECTION OF DIRECT PHOTOEFFECT

The probability of electromagnetic transition of a system from the initial state $|i\rangle$ to the final state $|f\rangle$ per unit time can be calculated within the time-dependent perturbation theory:

$$w = \frac{2\pi}{\hbar}|\langle f|H|i\rangle|^2\rho_f, \tag{18}$$

where the interaction operator H is expressed in terms of the nuclear current operator $\mathbf{j}(\mathbf{r})$ and the electromagnetic potential operator $\mathbf{A}(\mathbf{r})$, and ρ_f is the density of final states of the system.

If one limits oneself to consideration of only electric $E1$ and $E2$ transitions then by the use of this expression and the Siegert's theorem it can be shown (see the corresponding derivation in Ref. [18]) that the differential cross section of direct knockout of a nucleon from the orbit β of the target nucleus by a photon, corresponding to emission of a nucleon with the energy $\varepsilon = E_\gamma - B - E_n$ in the direction (θ, ϕ) with excitation of a given rotational state $|n\rangle$ of the final nucleus, can be expressed as

$$\frac{d\sigma_n(E_\gamma, \theta, \phi)}{d\Omega} = \frac{16\pi^3}{3}\frac{\mathcal{M}kE_\gamma}{c\hbar^3}\frac{e^2}{2(2J_0+1)} \times \sum_{\mu=\pm1}\sum_{s=\pm1/2}\sum_{M_nM_0}|\langle(\mathbf{k}s, n)^{(-)}|F_\mu|J_0M_0\rangle|^2, \tag{19}$$

where the operator F_μ is defined as

$$F_\mu = q_{\text{eff}}rY_{1\mu}(\vartheta, \varphi) + \left(\delta_{t_z-1/2} + O(A^{-1})\right) \times \frac{iE_\gamma}{\sqrt{20}c\hbar}r^2Y_{2\mu}(\vartheta, \varphi), \tag{20}$$

(r, ϑ, φ) are the spherical coordinates of the knocked out nucleon in the laboratory frame, q_{eff} is its effective electric charge for dipole excitation (equal to N/A for a proton and

$-Z/A$ for a neutron), t_z is the projection of the nucleon's isospin.

The cross section in Eq. (19) is averaged over possible values $\mu = \pm 1$ of the circular polarization of the photon beam and values of the quantum number M_0 of the target nucleus in the ground state and represents a sum over possible values of the z projection of spin ($s = \pm 1/2$) of the outgoing nucleon. It is seen from Eq. (20) that the quadrupole component of the electromagnetic field plays a significant role only in the case of direct knockout of protons with $t_z = -1/2$.

By substituting expansion (15) into Eq. (19) and performing summation over all magnetic quantum numbers we obtain the following expression for differential cross section:

$$\frac{d\sigma_n(E_\gamma,\theta,\phi)}{d\Omega} = D_1 + 2Re(D_{12})\delta_{t_z-1/2} + D_2\delta_{t_z-1/2}, \quad (21)$$

where

$$D_1 = \frac{2}{3}\frac{\pi^2 E_\gamma}{c\hbar}\frac{e^2 q_{\rm eff}^2}{2J_0+1}[A_0 + A_2 P_2(\cos\theta)], \quad (22)$$

$$D_{12} = -i\frac{2}{3}\frac{\pi^2}{\sqrt{20}}\frac{E_\gamma^2}{c^2\hbar^2}\frac{e^2 q_{\rm eff}}{2J_0+1}[A_1 P_1(\cos\theta) + A_3 P_3(\cos\theta)], \quad (23)$$

$$D_2 = \frac{\pi^2}{30}\frac{E_\gamma^3}{c^3\hbar^3}\frac{e^2}{2J_0+1}[B_0 + B_2 P_2(\cos\theta) + B_4 P_4(\cos\theta)]. \quad (24)$$

The coefficients A_0 and B_0 determine the angle-integrated differential cross section of the direct photoelectric effect. The remaining coefficients A_1, A_2, A_3, B_2, and B_4 describe the angular distribution of outgoing knocked out nucleons. Expressions for their calculation are given in the Appendix. The first term on the right-hand side of the expression (21) takes into account the contribution of the $E1$ transitions to the cross section, the second one the effect of interference of $E1$ and $E2$ transitions, the third one the contribution of $E2$ transitions. From Eqs. (21)–(24) it follows that the angular distribution of the nucleons produced by the direct knockout does not depend on the azimuthal angle ϕ in the laboratory frame, the z axis of which is directed along the direction of the incident photon.

V. SYSTEM OF COUPLED-CHANNEL EQUATIONS

From Eqs. (21)–(24), (A1)–(A11) it follows that in order to calculate the cross section $d\sigma_n(E_\gamma,\theta,\phi)/d\Omega$, corresponding to knockout of a nucleon from the orbit $(\beta\Omega)$ with the energy $\varepsilon = E_\gamma - B - E_n$ in the direction (θ,ϕ) and to production of the final nucleus in the state $|n\rangle$ of a given rotational band, it is necessary to calculate the components $\langle(\alpha,n)_J^{(-)}|(N'l'j',n')_J\rangle = \langle(\alpha,n)_{JM}^{(-)}|(N'l'j',n')_{JM}\rangle$ of the scattering state $|(\alpha,n)_{JM}^{(-)}\rangle$, where $|N'l'j'm'\rangle$ are the single-nucleon states in the spherical harmonic oscillator potential in the laboratory frame and $|n'\rangle$ are the final nucleus states from the same rotational band as the $|n\rangle$ state. Multiplying on the right the conjugate equation of Eq. (16) by $|(N'l'j',n')_{JM}\rangle$ we obtain

$$\langle(\alpha,n)_{JM}^{(-)}|(N'l'j',n')_{JM}\rangle = \langle(\alpha,n)_{JM}|(N'l'j',n')_{JM}\rangle + \langle(\alpha,n)_{JM}^{(-)}|V\frac{1}{\varepsilon+E_n-H_0+i\rho}\times|(N'l'j',n')_{JM}\rangle. \quad (25)$$

Further,

$$\langle(\alpha,n)_{JM}|(N'l'j',n')_{JM}\rangle = \delta_{n'n}\delta_{l'l}\delta_{j'j}\langle\varepsilon l|N'l\rangle, \quad (26)$$

where $\langle\varepsilon l|N'l\rangle$ is the scalar product of the wave function $\langle r|\varepsilon l\rangle = \sqrt{\frac{2k\mathcal{M}}{\hbar^2\pi}}\,j_l(kr)$ describing free motion of nucleon with the energy ε and orbital angular momentum l and the radial spherical harmonic oscillator function.

With the help of the basis states $\{|(Nlj,n)_{JM}\rangle\}$ and $\{|(\alpha,n)_{JM}\rangle \equiv \{|(\varepsilon lj,n)_{JM}\rangle\}$, which correspond to a given rotational band of the final nucleus, excited in the process of the nucleon knockout, the second term of the right-hand side of Eq. (25) can be expressed as

$$\langle(\alpha,n)_{JM}^{(-)}|V\frac{1}{\varepsilon+E_n-H_0+i\rho}|(N'l'j',n')_{JM}\rangle = \sum_{N''l''j''n''}\langle(\alpha,n)_{JM}^{(-)}|(N''l''j'',n'')_{JM}\rangle\int_0^\infty\langle(N''l''j'',n'')_{JM}|V|(\tilde{\varepsilon}l'j',n')_{JM}\rangle\langle\tilde{\varepsilon}l'|N'l'\rangle\frac{d\tilde{\varepsilon}}{\varepsilon+E_n-\tilde{\varepsilon}-E_{n'}+i\rho}. \quad (27)$$

Substituting expressions (26)–(27) into Eq. (25) and using relations (7), (8) we obtain, after simple transformations, a system of algebraic coupled-channel equations that allows one to find the components of the scattering state $|(\alpha,n)_J^{(-)}\rangle$ with the energy $E = \varepsilon + E_n$ and total angular momentum J, corresponding to emission of a nucleon with the energy ε, orbital momentum l, and total angular momentum j and to formation of the final nucleus in the nth state of the rotational band associated with it in the process of direct knockout of a nucleon from a given orbit of the target nucleus by a photon with the energy E_γ:

$$\sum_{N''l''j''n''} W_{N'l'j'n',N''l''j''n''}(E_\gamma,n,J,\beta,K)\,\langle(\alpha n)_J^{(-)}|(N''l''j'',n'')_J\rangle = -\delta_{ll'}\delta_{jj'}\delta_{nn'}\langle\varepsilon l|N'l\rangle. \quad (28)$$

The matrix of the system of coupled-channel equations is explicitly given by the expression

$$W_{N'l'j'n',N''l''j''n''}(E_\gamma, n, J, \beta, K) = \sum_\lambda \left[A(l''j''n''l'j'n'\lambda; KJ) P \int_0^\infty \frac{\langle N''l''|v_\lambda(r)|\tilde{\varepsilon}l'\rangle\langle\tilde{\varepsilon}l'|N'l'\rangle d\tilde{\varepsilon}}{\varepsilon + E_n - \tilde{\varepsilon} - E_{n'}} - i\pi(\langle N''l''|v_\lambda(r)|\tilde{\varepsilon}l'\rangle\langle\tilde{\varepsilon}l'|N'l'\rangle)_{\tilde{\varepsilon}=\varepsilon+E_n-E_{n'}} \right] + B(l''j''n''l'j'n') \left[P \int_0^\infty \frac{\langle N''l''|\frac{1}{r}\frac{df_s(r)}{dr}|\tilde{\varepsilon}l'\rangle\langle\tilde{\varepsilon}l'|N'l'\rangle d\tilde{\varepsilon}}{\varepsilon + E_n - \tilde{\varepsilon} - E_{n'}} - i\pi(\langle N''l''|\frac{1}{r}\frac{df_s(r)}{dr}|\tilde{\varepsilon}l'\rangle\langle\tilde{\varepsilon}l'|N'l'\rangle)_{\tilde{\varepsilon}=\varepsilon+E_n-E_{n'}} \right] - \delta_{N''N'}\delta_{l''l'}\delta_{j''j'}\delta_{n''n'}., \quad (29)$$

where the symbol $P\int \ldots d\tilde{\varepsilon}$ denotes the Cauchy principal value of the integral,

$$A(l''j''n''l'j'n'\lambda; KJ) \equiv \frac{1}{\sqrt{4\pi}}(-1)^{J-I_{n'}+I_{n''}-K-1/2}\hat{I}_{n'}\hat{l}'\hat{j}'\hat{I}_{n''}\hat{l}''\hat{j}''\hat{\lambda} \begin{pmatrix} I_{n''} & \lambda & I_{n'} \\ K & 0 & -K \end{pmatrix} \begin{pmatrix} l'' & \lambda & l' \\ 0 & 0 & 0 \end{pmatrix} \begin{Bmatrix} j'' & \lambda & j' \\ l' & \frac{1}{2} & l'' \end{Bmatrix} \begin{Bmatrix} J & I_{n'} & j' \\ \lambda & j'' & I_{n''} \end{Bmatrix} \quad (30)$$

[where for brevity we use the notation $\hat{a} = (2a+1)^{1/2}$],

$$B(l''j''n''l'j'n') \equiv \delta_{n''n'}\delta_{l''l'}\delta_{j''j'}(U_s + iW_s)\left(\frac{\hbar}{m_\pi c}\right)^2 \times [j'(j'+1) - l'(l'+1) - 3/4], \quad (31)$$

U_s and W_s are the values of the real and imaginary parts of the depth of the spin-orbit potential, m_π is the π meson mass, $f_s(r) = \{1 + \exp[(r - R_s)/a_s]\}^{-1}$ is the form factor of the spin-orbit interaction.

It should be noted that the conservation of parity and total angular momentum conditions significantly reduce the number of dimensions of the system of equations (28). In fact, for heavy even-even nuclei and with $N_{\max} = 30$, it does not exceed 300.

The cross section (19) describes a single reaction channel with a definite total angular momentum J corresponding to knockout of a nucleon from a given single-particle state $|\beta\Omega\rangle$ of the target nucleus resulting in excitation of a given state (n) of the rotational band of the final nucleus built on the produced nucleon hole excitation. In order to obtain the total cross section of nucleon knockout from the selected orbit one has to perform summation of the cross section (19) over all possible values of J and n and multiply by a factor of 2, if the orbit is occupied by two nucleons. For calculation of the total cross section of nucleon knockout all near-surface orbits giving a significant contribution to it have to be considered.

VI. APPLICATION OF THE MODEL TO ^{108}Pd, ^{160}Gd, ^{184,186}W, ^{180}Hf

In the considered energy range ($E_\gamma \lesssim 40$ MeV) the yield of direct photoneutrons in (γ, n) reactions comprises only a small fraction of the photoneutron yield resulting from the statistical decay of the giant dipole resonance (GDR) and is hard to detect in the experimental data. For this reason the model described in the previous sections is applied in this work only to description of the reaction of direct knockout of protons from heavy deformed nuclei, for which experimental data on the photoproton yield at these energies are available in literature.

Unfortunately, there is not much data on photoproton reactions in the specified region of nuclei and energies that can be used to test the model. The most useful measurements for this purpose are presented in the works [28–30] where the cross sections of the (γ, p) reaction were obtained on ^{108}Pd, ^{160}Gd, and ^{184,186}W at $E_\gamma \lesssim 32$ MeV using the activation technique.

The calculations for these nuclei were performed in the energy range from the (γ, p) reaction threshold to $E_\gamma = 40$ MeV with the step size $h = 1$ MeV. Parameters of the components of the complex potential V—the values of the radius, diffuseness parameter, and depth of the potential well (fixed at the energy of the scattered particle corresponding to the maximum of the experimental cross section)—were taken from the global optical model [22]. The quadrupole deformation parameters of ^{108}Pd, ^{160}Gd, ^{184,186}W were estimated from the compilation of experimental static quadrupole moments [31].

As the calculations show, in order to compensate the deficit of the theoretical cross section of $\sigma(\gamma, p)$ at $E_\gamma \approx 23$ MeV for the considered nuclei it is enough to take into account the direct knockout of photoprotons from several orbits closest to the Fermi surface. Thus, for the ^{160}Gd and ^{184}W isotopes, whose quadrupole deformation parameters δ are, respectively, 0.335 and 0.241, the calculations considered direct knockout from six near-surface proton orbits, and for ^{108}Pd and ^{186}W ($\delta = 0.15$ and $\delta = 0.201$, respectively) five orbits were considered.

The Coriolis and centrifugal forces affect significantly the internal structure of a rotating nucleus, which may lead to breaking of the adiabatic condition at high I. For this reason the maximum number of the considered rotational band levels was limited by the parameter $n_{\max}$. The value of this parameter as well as the moment of inertia of the final nucleus ($\mathcal{T}$) were estimated from the available spectra of the rotational bands of the final nucleus in the ENSDF database [32–36]. For ^{160}Gd the values of these parameters were taken as $\hbar^{-2}\mathcal{T} = 50$ MeV^{-1} and $n_{\max} = 5$ for the ^{184,186}W isotopes $\hbar^{-2}\mathcal{T} = 31$ MeV^{-1} and $n_{\max} = 4$, and for the ^{108}Pd nucleus $\hbar^{-2}\mathcal{T} = 16$ MeV^{-1} and $n_{\max} = 5$.

In the expansion (7) of the potential V into spherical harmonics the values $\lambda = 0, 2, 4, 6$ of the orbital quantum

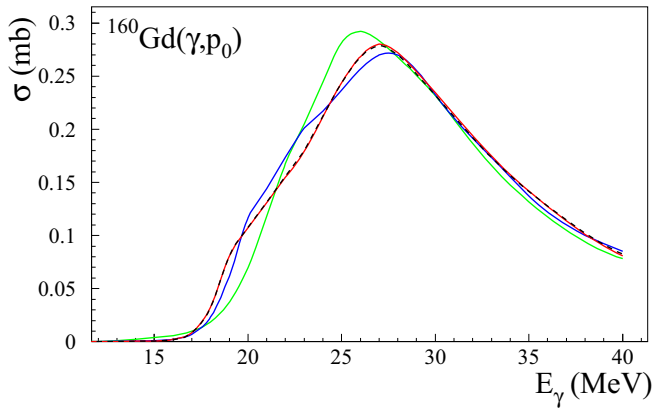

FIG. 1. Cross section of direct γ-induced knockout of a proton from ^{160}Gd for transition into the ground state of the final nucleus. Green, blue, and red curves correspond to the values of $\varepsilon_{\max} = 100$ MeV and $N_{\max} = 20$, 25, and 30, respectively, and black dashed curve to $\varepsilon_{\max} = 150$ MeV and $N_{\max} = 30$.

number were used. The bound single-particle states of the target nucleus $|\beta\rangle$, from which the protons are knocked out, were calculated, as noted previously, using the model described in Ref. [23]. The single-particle basis states $|Nljm\rangle$ are calculated in the oscillatory spherical potential with $\hbar\omega = 41A^{-1/3}$ MeV.

Important parameters of the model are the constants $N_{\max}$ and $\varepsilon_{\max}$ that limit the configuration space of the basis states $\{|(Nlj, n)_{JM}\rangle\}$ and $\{|(\alpha, n)_{JM}\rangle \equiv \{|(\varepsilon lj, n)_{JM}\rangle\}$ used in Eq. (27) for transformation of the integral equations (25) into the algebraic system (28). The values of these parameters have to be sufficiently large for reliability and stability of the calculations.

Figure 1 shows the results of computation of the direct component of the cross section of the ^{160}Gd(γ, p_0) reaction (corresponding to proton knockout from the Fermi level) for different values of $\varepsilon_{\max}$ and $N_{\max}$: green, blue, and red curves correspond to the values of $\varepsilon_{\max} = 100$ MeV and $N_{\max} = 20$, 25, and 30, respectively, and black dashed curve to $\varepsilon_{\max} = 150$ MeV and $N_{\max} = 30$. Taking into consideration the rapid increase of the computation time as a function of $N_{\max}$ and the relatively small difference between the blue and red curves, one can conclude that the value $N_{\max} = 30$ is close to optimal. Therefore, the subsequent calculations were performed with this value of the parameter $N_{\max}$. As also seen from the figure, the black dashed curve is almost indistinguishable from the red one, indicating that setting $\varepsilon_{\max} = 100$ MeV is reliable enough for further calculations.

Comparison of the calculated cross sections of direct proton knockout with the experimental data also requires calculation of the statistical component of the photoproton reaction, since only the total reaction cross sections were obtained in the mentioned experiments. For this purpose results of calculations of two implementations of the statistical model were used: the TALYS nuclear reaction simulation package [37] (using the data published in the TENDL-2021 database [38]) and the combined model of photonuclear reactions (CMPR) [39]. Both models contain description of the preequilibrium (using the exciton model) and evaporation (using the Bohr compound nucleus picture) phases of photonuclear reactions, but the CMPR model additionally takes into account important aspects of photonuclear reactions, namely, the effects of the nuclear deformation, structure of the doorway excitation state of the GDR and isospin dependence of its decay channels.

Figure 2 shows the comparison of the obtained results with the experimental data for the cross section of the (γ, p) reaction on the ^{160}Pd, ^{160}Gd, and ^{184,186}W isotopes. The experimental cross section of (γ, p) is shown with black dots with statistical error bars for ^{160}Gd [28] and ^{108}Pd [30] and with black dashed curve with points for the ^{184}W and ^{186}W nuclei [29]. Continuous curves show the results of the theoretical calculation of different components of this cross section: the red curve shows the proton DKO cross section calculated using the described model; the blue and purple curves correspond to the statistical component of the (γ, p) reaction cross section, calculated, respectively, using the CMPR and TALYS models, both with default parameters; the black curve shows the sum of the statistical (CMPR) and direct components of the (γ, p) cross section (i.e., the sum of the red and blue curves); and, for comparison, the green curve denotes the proton DKO cross section without the described effect of interaction with the rotational states of the final nucleus, ignoring the excited states of rotational bands by setting $n_{\max} = 1$.

It should be noted that the experimental cross sections $\sigma(\gamma, p)$ shown in Fig. 2 represent practically all known (at least to us) data on measured photoproton cross sections for heavy deformed nuclei at $E_\gamma \lesssim 40$ MeV. In addition to this, in a number of works yields of photoproton reactions induced by bremsstrahlung photon beams on suitable targets were measured. However, due to the continuous spectrum of bremsstrahlung radiation usage of such data is generally limited only to those cases where detailed information about the conditions of irradiation can be obtained to reproduce the energy distribution of the incident photons. This information was available for the measurement of the (γ, p) reaction yield on ^{180}Hf in the bremsstrahlung photon beam with the maximum energy $E_{\gamma\,\max} = 55$ MeV with the photon activation technique [40]. The measured value of the total photoproton reaction yield was equal to $Y_{\exp} = (2.09 \pm 0.21) \times 10^{-7}$ $1/e$, where the $1/e$ units denote the number of (γ, p) reactions per one incident electron.

We calculated the direct component of the ^{180}Hf(γ, p) ^{179}Lu reaction cross section from the reaction threshold up to 55 MeV, assuming the possibility of the proton knock out from six near-surface single-particle orbits and excitation of $n_{\max} = 4$ lowest rotational states of the resulting final nucleus, and using the parameter values $\delta = 0.265$ and $\hbar^{-2}\mathcal{T} = 37$ MeV^{-1}. The statistical component of the reaction cross section was calculated using the CMPR and the TALYS models. The theoretical yield Y corresponding to these reaction channels was obtained by folding the cross sections with the bremsstrahlung photon spectrum calculated using a GEANT4 [41] simulation. As a result, the value $Y_{\text{DKO}} = 0.70 \times 10^{-7}$ $1/e$ was obtained for the direct proton knockout yield, and $Y_{\text{CMPR}} = 2.00 \times 10^{-7}$ $1/e$ for the statistical yield using the combined model, and

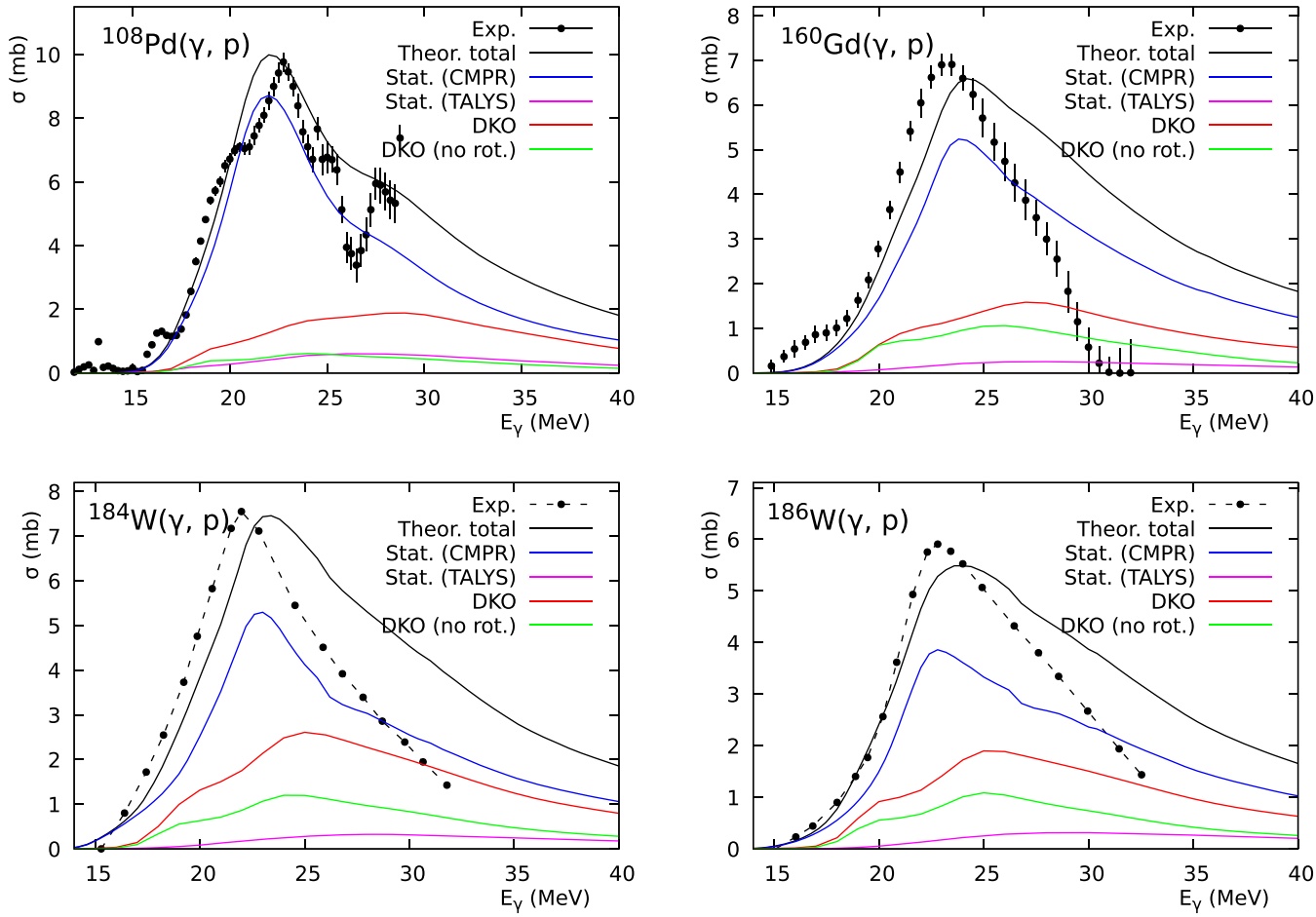

FIG. 2. Cross sections of the (γ, p) reaction on ^{108}Pd, ^{160}Gd, and ^{184,186}W. Experiment: black points [28–30]. Theory: red curve, contribution of the proton DKO with coupling with rotational band states ($n = 1, 2, \ldots, n_{\max}$); green curve, contribution of the DKO without this coupling ($n = 1$); contribution of the processes involving formation of the compound nucleus is shown as blue (CMPR model [39]) and purple curves (TALYS calculation from the TENDL database [38]); black curve, total contribution of the direct and statistical reaction mechanisms.

$Y_{\text{TALYS}} = 7.94 \times 10^{-9}\ 1/e$ when using the TALYS program. In addition, Fig. 3 shows the differential cross sections of the direct proton knockout from ^{108}Pd, ^{160}Gd, ^{184}W, and ^{186}W calculated at the energies $E_\gamma = 13$–38 MeV.

VII. DISCUSSION OF THE RESULTS

It is seen from Fig. 2 that the DKO cross section of the (γ, p) reaction calculated using the described model provides about 30% of the total experimental reaction cross section on all of the considered nuclei, which represents an improvement in comparison with the previous version of the model (see Ref. [19] and the corresponding erratum), which assumed that the proton knockout in the course of the surface direct nuclear photoeffect takes place solely from the Fermi level with no interaction with the rotational band of the final nucleus. Specifically, the peak values of the proton DKO cross sections in the previous version of the model were equal to 0.48, 0.20, and 0.25 mb on, respectively, ^{160}Gd, ^{184}W, and ^{186}W. Hence, in the updated calculation the improvement amounts to a factor of 3 for ^{160}Gd and to a factor of about 10 for the isotopes of tungsten. Comparison of red and green curves in Fig. 2, corresponding to DKO cross section with and without excitation of the rotational band, shows that the interaction of the knocked out proton with the rotational degree of freedom of the final deformed nucleus approximately doubles the cross section of direct photoeffect.

It is immediately noticeable from the figure and also from the reaction yields on ^{180}Hf that the statistical component of the total reaction cross section calculated by TALYS is underestimated by over an order of magnitude. Such behavior is not surprising as it is known that a baseline statistical model will often underestimate the yield of photoprotons in photonuclear reactions on medium and heavy nuclei in the energy range of the giant dipole resonance (see, e.g., Refs. [42–45]). Indeed, in addition to the Coulomb barrier, two principal factors also affect the competition between the photoproton and photoneutron decay channels of the GDR. Namely, on the one hand, the isospin selection rules result in predominant emission of protons from the $T_>$ branch of the GDR.

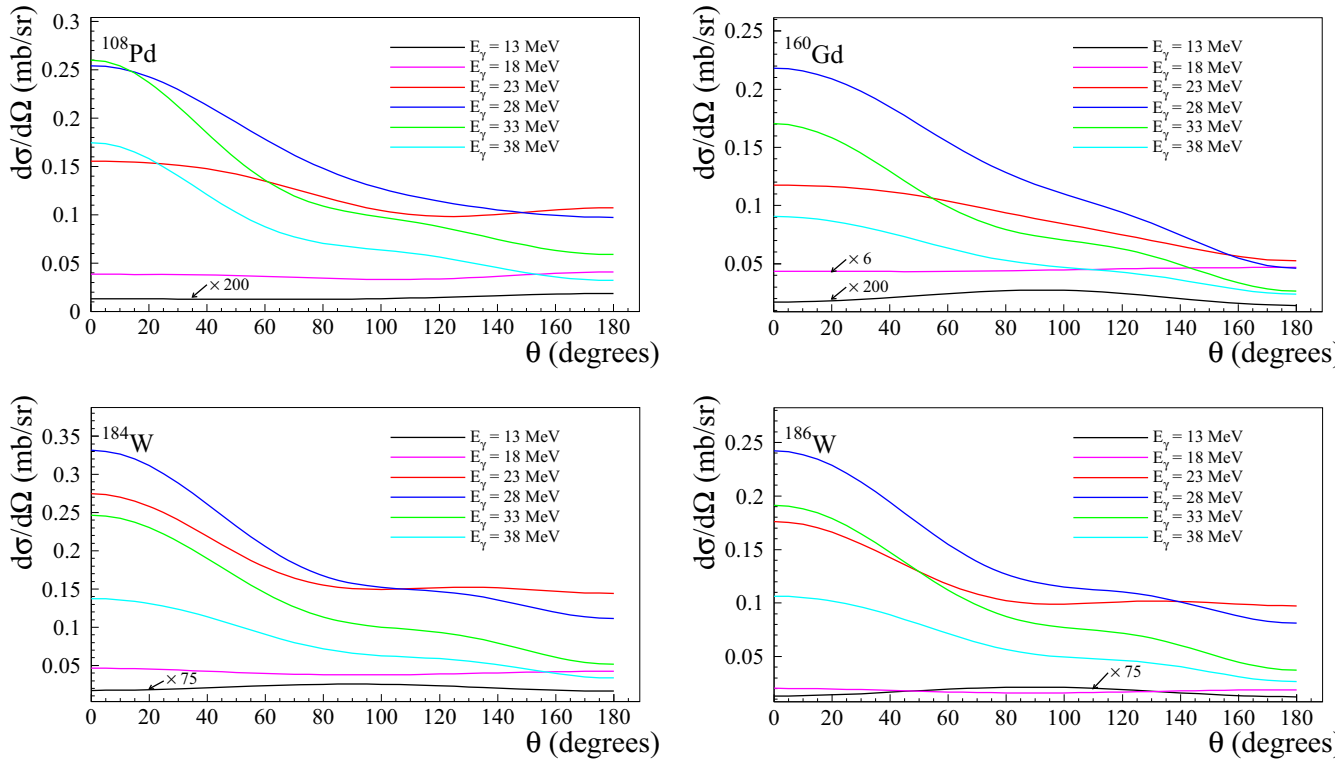

FIG. 3. Differential cross sections of the direct proton knockout reaction from ^{108}Pd, ^{160}Gd, and ^{184,186}W, calculated at $E_\gamma = 13$ MeV (black), $E_\gamma = 18$ MeV (purple), $E_\gamma = 23$ MeV (red), $E_\gamma = 28$ MeV (blue), $E_\gamma = 33$ MeV (green), $E_\gamma = 38$ MeV (cyan).

On the other hand, the energy of the collective shift of the resonance is carried away by outgoing semidirect nucleons already in the early stages of the decay, resulting in enhancement of the yield of high-energy particles, which, in turn, reduces inhibition of the photoproton yield by the Coulomb barrier. Both of these factors are approximately taken into account by the CMPR model [39], and, as can be seen from the figure, the obtained statistical cross sections are in line with the data. For this reason, the CMPR cross sections were used for calculation of the total (γ, p) reaction cross sections.

The direct photoeffect results in a noticeable contribution to the total cross section of the (γ, p) reaction. Specifically, enabling of the direct proton knockout mechanism allowed us to compensate the lack of the statistical photoproton yield and reproduce the amplitude of the total cross section in the considered energy range. However, the maximum of the total theoretical cross section $\sigma(\gamma, p) = \sigma^{\mathrm{CMPR}}(\gamma, p) + \sigma^{\mathrm{DKO}}(\gamma, p)$ is shifted towards larger energies for ^{160}Gd, ^{184,186}W with respect to the experimental cross section by approximately 2 MeV, and its decrease at large energies E_γ is significantly less steep.

The calculated DKO cross section on ^{160}Gd is noticeably less than on ^{184}W, while the number of close-to-surface orbits taken into account in the DKO calculation was equal. Two factors can provide an explanation. On the one hand the kinetic energy of nucleons knocked out from ^{160}Gd is less than in the case of ^{184,186}W due to the larger proton separation threshold in this nucleus ($B_p = 9.19$ MeV in ^{160}Gd and 7.70 MeV in ^{184}W). This, evidently, assists in increase of the yield of direct photoprotons from ^{184}W compared to ^{160}Gd, as more energetic outgoing particles leave the interaction region more rapidly, preventing their capture into the compound nucleus. On the other hand, the heavier nuclei with a larger surface area have a larger probability to find near it a proton in one of the concerned orbits. Since the nucleons knocked out from the surface are less subject to the effect of the absorption terms of the average field responsible for formation of the compound nucleus, they give a larger contribution to the direct photoeffect, other things being equal. This aspect, in fact, is the basis of the assumption of the surface nature of the direct photoeffect on heavy deformed nuclei in the considered energy range.

The energy dependence of the direct photoeffect cross section for the considered nuclei is of a significant interest. As seen from Fig. 2 they change very slowly with the energy E_γ, slower than the cross sections of partial photonucleon reactions in the energy range $E_\gamma \lesssim 20$ MeV, producing a broad pseudoresonance with a maximum at about $E_\gamma \approx 25$–30 MeV. In order to clarify the nature of this situation we refer to the result of calculation of angular distributions of outgoing direct photoprotons at different energies E_γ, shown in Fig. 3. As seen from these figures, at small energies of the incident photon ($E_\gamma < 20$ MeV) the angular distribution of the outgoing direct protons is close to isotropic. However, as the E_γ energy increases it becomes asymmetric, with a large predominance of the number outgoing protons in the forward direction. Such behavior of the angular distribution results in a situation when

the number of the knocked out protons that could leave the reaction region without formation of a compound nucleus first increases with increase of the photon energy E_γ, and then begins to decrease due to the prevailing forward direction of protons knocked out from the frontal side of the surface having to travel through the bulk of the nuclear matter, where their energy is distributed among other nucleons with increasingly larger probability.

It also follows from Fig. 2 that for ^{160}Gd, ^{184,186}W the theoretical integrated cross section of the (γ, p) reaction evaluated in the interval from the reaction threshold B_p to $E_{\gamma_{\max}} \gtrsim 28$ MeV is larger than the corresponding experimental cross section, which is a result of a slower decrease of the statistical and direct components of the theoretical cross section at large energies E_γ compared to the experimental cross section.

This disagreement of the theory and experiment at the high-energy tail of the reaction cross sections can, of course, be a result of systematic uncertainties of both the direct proton knockout model and the predictions of the CMPR based on formation and decay of the GDR, whose behavior far away from the maximum of photoabsorption is still poorly known. However, it should be noted that the accuracy of photonuclear cross sections is sometimes not very high [46]. Bremsstrahlung radiation was used as a photon source in the experiments on all considered nuclei, and, therefore, artifacts could be introduced during reconstruction of the reaction cross sections as a function of E_γ. In Ref. [28] above 25 MeV the β activity from ^{159}Eu could not be separated from ^{158}Eu and the ^{160}Gd (γ, p) ^{159}Eu reaction cross section is a result of estimation. The uncertainty of the integrated cross sections on ^{184,186}W was estimated by the authors in Ref. [29] to be of the order of 20%.

On the other hand the theoretical value $Y^{\mathrm{CMPR}} + Y^{\mathrm{DKO}}$ of the photoproton yield from ^{180}Hf in the $E_{\gamma_{\max}} = 55$ MeV bremsstrahlung photon beam also displays an excess of approximately 30% over the experimental yield measured in Ref. [40], which again can indicate overestimation of the calculated (γ, p) cross section in the high-energy tail of the GDR.

In conclusion we note certain directions of further development of the model. First, introduction of the effect of pairing interaction can lead to a better agreement with the data. Indeed, within the BCS model of the nucleon pairing effect the incident photon should find paired nucleons in the single-particle levels of the deformed average field at the energies greater than the Fermi energy, which will shift the direct photoeffect curve to the left.

Second, for photoabsorption on heavy nuclei one can, in principle, to a certain degree increase the energy limit $E_{\max} \approx 40$ MeV at which the described nonrelativistic version of the DKO on deformed nuclei can still be applied. This increase cannot be large—at most up to 60–80 MeV—due to the limitations arising from the usage of the Siegert's theorem (see estimates made in Sec. I). A natural question then is whether the described model can be further developed so as to successfully describe the nuclear photoeffect on deformed nuclei, or at least a significant part of it, at larger energies, and whether it can be done while staying within the framework of DKO, since the presented formalism assumes that the outgoing nucleon interacts with the rotational states of the final nucleus built on the hole excitations produced after the absorption of the photon by a single nucleon.

Evidently, the desired result cannot be achieved within the nonrelativistic approach, since, as mentioned in Sec. I, the contribution of the nonrelativistic mechanism of the DKO to the total cross section of the (γ, p) reaction is usually very small even at moderate energies and in the case of the (γ, n) reaction it is negligible even at low energies [7].

On the other hand, relativistic calculations reveal a significant contribution of the DKO mechanism in the (γ, p) cross section up to the energies of $E \approx 500$ MeV. One can hope, therefore, that consideration of the relativistic effects (e.g., using the formalism developed in Ref. [4]) will allow us to extend the energy range of the presented model. At the same time, for this problem to be tackled in practice it is desirable that experimental data on photonucleon reactions on heavy deformed nuclei at large energies become available.

ACKNOWLEDGMENTS

We acknowledge our sincere thankfulness to Prof. V. V. Varlamov (SINP MSU) for his help and useful remarks during discussion of this work.

APPENDIX: COEFFICIENTS OF LEGENDRE POLYNOMIALS EXPANSION OF D_1, D_{12}, AND D_2

The coefficients describing the expansion of the differential cross section (21) into Legendre polynomials [see Eqs. (22)–(24)] are determined by the following expressions (hereafter the notation $\hat{a} = \sqrt{2a+1}$ is used for brevity):

$$A_0 = \frac{2}{3}\sum_{ljJ} |\langle (\alpha, n)^{(-)}_J \parallel rY_1(\vartheta, \varphi) \parallel J_0\rangle|^2, \tag{A1}$$

$$A_1 = \frac{6}{\sqrt{10}}(-1)^{I_n+1/2+J_0}\sum_{lJl'j'J'}(-1)^{j+j'+J+J'}\hat{J}\hat{J}'\hat{j}\hat{j}'\hat{l}\hat{l}'\begin{pmatrix} l & l' & 1\\ 0 & 0 & 0\end{pmatrix}\begin{Bmatrix} j & 1 & j'\\ l' & \frac{1}{2} & l\end{Bmatrix}\begin{Bmatrix} 1 & J & J'\\ I_n & j' & j\end{Bmatrix}\begin{Bmatrix} 1 & 1 & 2\\ J' & J_0 & J\end{Bmatrix}$$
$$\times \langle (\alpha, n)^{(-)}_J \parallel rY_1(\vartheta, \varphi) \parallel J_0\rangle\langle (\alpha', n)^{(-)}_{J'} \parallel r^2Y_2(\vartheta, \varphi) \parallel J_0\rangle^*|_{\varepsilon'=\varepsilon}, \tag{A2}$$

$$A_2 = -\sqrt{\frac{10}{3}}(-1)^{I_n+1/2+J_0}\sum_{lJl'j'J'}(-1)^{j+j'+J+J'}\hat{J}\hat{J}'\hat{j}\hat{j}'\hat{l}\hat{l}'\begin{pmatrix} l & l' & 2\\ 0 & 0 & 0\end{pmatrix}\begin{Bmatrix} j & 2 & j'\\ l' & \frac{1}{2} & l\end{Bmatrix}\begin{Bmatrix} 2 & J & J'\\ I_n & j' & j\end{Bmatrix}\begin{Bmatrix} 1 & 2 & 1\\ J' & J_0 & J\end{Bmatrix}$$
$$\times \langle (\alpha, n)^{(-)}_J \parallel rY_1(\vartheta, \varphi) \parallel J_0\rangle\langle (\alpha', n)^{(-)}_{J'} \parallel rY_1(\vartheta, \varphi) \parallel J_0\rangle^*|_{\varepsilon'=\varepsilon}. \tag{A3}$$

$$A_3 = 2\sqrt{\frac{7}{5}}(-1)^{I_n+1/2+J_0}\sum_{ljJl'j'J'}(-1)^{j+j'+J+J'}\hat{j}\hat{j}'\hat{j}\hat{j}'\hat{l}\hat{l}'\begin{pmatrix} l & l' & 3\\ 0 & 0 & 0\end{pmatrix}\begin{Bmatrix} j & 3 & j'\\ l' & \frac{1}{2} & l\end{Bmatrix}\begin{Bmatrix} 3 & J & J'\\ I_n & j' & j\end{Bmatrix}\begin{Bmatrix} 1 & 3 & 2\\ J' & J_0 & J\end{Bmatrix}$$
$$\times\langle(\alpha,n)^{(-)}_J \parallel rY_1(\vartheta,\varphi)\parallel J_0\rangle\langle(\alpha',n)^{(-)}_{J'}\parallel r^2Y_2(\vartheta,\varphi)\parallel J_0\rangle^*|_{\varepsilon'=\varepsilon}. \tag{A4}$$

$$B_0 = \frac{2}{5}\sum_{ljJ}|\langle(\alpha,n)^{(-)}_J\parallel r^2Y_2(\vartheta,\varphi)\parallel J_0\rangle|^2, \tag{A5}$$

$$B_2 = -2\sqrt{\frac{5}{14}}(-1)^{I_n+1/2+J_0}\sum_{ljJl'j'J'}(-1)^{j+j'+J+J'}\hat{j}\hat{j}'\hat{j}\hat{j}'\hat{l}\hat{l}'\begin{pmatrix} l & l' & 2\\ 0 & 0 & 0\end{pmatrix}\begin{Bmatrix} j & 2 & j'\\ l' & \frac{1}{2} & l\end{Bmatrix}\begin{Bmatrix} 2 & J & J'\\ I_n & j' & j\end{Bmatrix}\begin{Bmatrix} 2 & 2 & 2\\ J' & J_0 & J\end{Bmatrix}$$
$$\times\langle(\alpha,n)^{(-)}_J \parallel r^2Y_2(\vartheta,\varphi)\parallel J_0\rangle\langle(\alpha',n)^{(-)}_{J'}\parallel r^2Y_2(\vartheta,\varphi)\parallel J_0\rangle^*|_{\varepsilon'=\varepsilon}, \tag{A6}$$

$$B_4 = -12\sqrt{\frac{2}{35}}(-1)^{I_n+1/2+J_0}\sum_{ljJl'j'J'}(-1)^{j+j'+J+J'}\hat{j}\hat{j}'\hat{j}\hat{j}'\hat{l}\hat{l}'\begin{pmatrix} l & l' & 4\\ 0 & 0 & 0\end{pmatrix}\begin{Bmatrix} j & 4 & j'\\ l' & \frac{1}{2} & l\end{Bmatrix}\begin{Bmatrix} 4 & J & J'\\ I_n & j' & j\end{Bmatrix}\begin{Bmatrix} 2 & 4 & 2\\ J' & J_0 & J\end{Bmatrix}$$
$$\times\langle(\alpha,n)^{(-)}_J \parallel r^2Y_2(\vartheta,\varphi)\parallel J_0\rangle\langle(\alpha',n)^{(-)}_{J'}\parallel r^2Y_2(\vartheta,\varphi)\parallel J_0\rangle^*|_{\varepsilon'=\varepsilon}. \tag{A7}$$

As seen from Eqs. (21)–(24), (A1)–(A7) calculation of the cross section $d\sigma_n(E_\gamma,\theta,\phi)/d\Omega$ requires evaluation of the reduced matrix elements $\langle(\alpha,n)^{(-)}_J\parallel r^LY_L(\vartheta,\varphi)\parallel J_0\rangle$, where $L=1,2$. By expanding the scattering state $|(\alpha,n)^{(-)}_{JM_0}\rangle$ into $|(N'l'j',n')_{JM_0}\rangle$ states, where $|N'l'j'm'\rangle$ are the spherical harmonic oscillator eigenstates in the laboratory frame with $\hbar\omega = 41A^{-1/3}$ MeV and $|n'\rangle$ are the final nucleus's states from the same rotational band as the $|n\rangle$ state, we obtain

$$\langle(\alpha,n)^{(-)}_{JM_0}|r^LY_{L0}(\vartheta,\varphi)|J_0M_0\rangle = \sum_{N'l'j'm'n'}\langle(\alpha,n)^{(-)}_{JM_0}|(N'l'j',n')_{JM_0}\rangle(j'm'I_{n'}M_{n'}|JM_0)\langle N'l'j'm',n'|r^LY_{L0}(\vartheta,\varphi)|J_0M_0\rangle. \tag{A8}$$

The quantity of interest is the amplitude of transition of a nucleon from a bound single-particle state $|\beta\Omega\rangle$ of the target nucleus to the continuum scattering state. In the intrinsic frame the bound single-particle states were calculated by diagonalization of the single-particle Hamiltonian using a deformed Woods-Saxon potential described in Ref. [23] in the spherical harmonic oscillator basis $\{|N_0l_0j_0\Omega\rangle\}$. In this way the wave function $\varphi'_{\beta\Omega}$ entering the ground state of the target nucleus in Eq. (1) is expressed in the form

$$\varphi'_{\beta\Omega} = \sum_{N_0l_0j_0}C_{N_0l_0j_0}(\beta\Omega)|N_0l_0j_0\Omega\rangle, \tag{A9}$$

where $C_{N_0l_0j_0}(\beta\Omega)$ are the coefficients of expansion of the function $\varphi'_{\beta\Omega}$ into the spherical oscillator eigenfunctions in the intrinsic frame.

Using (1), (A8), and (A9) and the Wigner-Eckart theorem after a transformation we obtain

$$\langle(\alpha,n)^{(-)}_J\parallel r^LY_L(\vartheta,\varphi)\parallel J_0\rangle = \sum_{N'l'j'm'n'}\langle(\alpha,n)^{(-)}_J|(N'l'j',n')_J\rangle A(N'l'j'n';J_0JL\beta\Omega K), \tag{A10}$$

where

$$A(N'l'j'n';J_0JL\beta\Omega K) = \frac{1}{4\pi}(-1)^{\Omega+K+j'-I_{n'}}\hat{J}\hat{J}_0\hat{I}_{n'}\hat{L}\hat{l}'\hat{j}'\sum_{N_0l_0j_0}(-1)^{j_0+1/2}C_{N_0l_0j_0}(\beta\Omega)\hat{l}_0\hat{j}_0\begin{pmatrix} l' & L & l_0\\ 0 & 0 & 0\end{pmatrix}$$
$$\times\begin{pmatrix} I_{n'} & j_0 & J_0\\ K & \Omega & -\Omega-K\end{pmatrix}\begin{Bmatrix} j' & L & j_0\\ l_0 & \frac{1}{2} & l'\end{Bmatrix}\begin{Bmatrix} J & J_0 & L\\ j_0 & j' & I_{n'}\end{Bmatrix}\langle N'l'|r^L|N_0l_0\rangle. \tag{A11}$$

The radial matrix element $\langle N'l'|r^L|N_0l_0\rangle$ for oscillator functions can be calculated analytically [47].

[1] S. Boffi, C. Giusti, and F. Pacati, Nucl. Phys. A **359**, 91 (1981).

[2] G. van der Steenhoven and H. P. Blok, Phys. Rev. C **42**, 2597 (1990).

[3] J. Ryckebusch, K. Heyde, L. Machenil, D. Ryckbosch, M. Vanderhaeghen, and M. Waroquier, Phys. Rev. C **46**, R829 (1992).

[4] G. Lotz and H. Sherif, Nucl. Phys. A **537**, 285 (1992).

[5] D. Ireland, D. Branford, T. Davinson, N. Davis, E. Macdonald, P. Sellin, A. Shotter, P. Terzoudi, P. Woods, J.-O. Adler, B.-E. Anderson, L. Isaksson, D. Nilsson, H. Ruijter, A. Sandell, and B. Schröder, Nucl. Phys. A **554**, 173 (1993).

[6] D. G. Ireland and G. van der Steenhoven, Phys. Rev. C **49**, 2182 (1994).

[7] G. Benenti, C. Giusti, and F. Pacati, Nucl. Phys. A **574**, 716 (1994).

[8] I. Bobeldijk, C. Van den Abeele, J.-O. Adler, B.-E. Andersson, E. Aschenauer, L. de Bever, D. Branford, S. Bulychjov, T. Davinson, K. Hansen, D. Ireland, L. Isaksson, D. Ivanov, D. Johnstone, A. Khanov, L. Lapikás, L. Lindgren, G. de Meyer, B. Nilsson, H. Ruijter *et al.*, Phys. Lett. B **356**, 13 (1995).

[9] K. Mori, P. D. Harty, Y. Fujii, O. Konno, K. Maeda, I. Nomura, G. J. O'Keefe, J. Ryckebusch, T. Suda, T. Terasawa, M. N. Thompson, and Y. Torizuka, Phys. Rev. C **51**, 2611 (1995).

[10] G. Miller, J. McGeorge, J. Annand, G. Crawford, V. Holliday, I. MacGregor, R. Owens, J. Ryckebusch, J.-O. Adler, B.-E. Andersson, L. Isaksson, and B. Schrøder, Nucl. Phys. A **586**, 125 (1995).

[11] J. Johansson, H. Sherif, and G. Lotz, Nucl. Phys. A **605**, 517 (1996).

[12] J. I. Johansson and H. S. Sherif, Phys. Rev. C **56**, 328 (1997).

[13] E. Aschenauer, C. V. den Abeele, J.-O. Adler, B.-E. Andersson, L. de Bever, I. Bobeldijk, D. Branford, S. Bulychjov, T. Davinson, K. Hansen, D. Ireland, L. Isaksson, D. Ivanov, D. Johnstone, A. Khanov, L. Lapikás, L. Lindgren, G. de Meyer, D. V. Neck, B. Nilsson *et al.*, Nucl. Phys. A **615**, 33 (1997).

[14] A. Meucci, C. Giusti, and F. D. Pacati, Phys. Rev. C **64**, 064615 (2001).

[15] M. Anguiano, G. Co', A. Lallena, and S. Mokhtar, Ann. Phys. (NY) **296**, 235 (2002).

[16] C. Giusti and F. D. Pacati, Phys. Rev. C **67**, 044601 (2003).

[17] F. Pacati, C. Giusti, and A. Meucci, in *Nuclear Theory'22*, Vol. 22, edited by V. Nikolaev (Heron Press, Sofia, 2003), pp. 39–53.

[18] J. Eisenberg and W. Greiner, *Excitation Mechanisms of the Nucleus*, Nuclear theory: Three books (North-Holland, Amsterdam, 1988).

[19] B. S. Ishkhanov, V. N. Orlin, and K. A. Stopani, Phys. Rev. C **94**, 054623 (2016); **107**, 039902(E) (2023).

[20] A. Bohr and B. Mottelson, *Nuclear Structure*, Vol. 2 (W. A. Benjamin, New York, 1974).

[21] T. Tamura, Rev. Mod. Phys. **37**, 679 (1965).

[22] A. Koning and J. Delaroche, Nucl. Phys. A **713**, 231 (2003).

[23] G. I. Bykhalo, V. N. Orlin, and K. A. Stopani, arXiv:2107.08245.

[24] S. Sunakawa, *Quantum Scattering Theory* (Iwanami Shote, Tokyo, 1977; Mir, Moscow, 1979).

[25] J. R. Taylor, *Scattering Theory: The Quantum Theory on Nonrelativistic Collisions* (Wiley, New York, 1972).

[26] F. Villars, in *Fundamentals in nuclear theory; lectures presented at an International Course, Trieste, 3 October-16 December 1966*, edited by A. de-Shalit and C. Villi (International Atomic Energy Agency, Vienna, 1967), p. 269.

[27] L. Landau and E. Lifshitz, *Quantum Mechanics*, 3rd ed. (Pergamon, Oxford, 1977).

[28] F. Dreyer, H. Dahmen, J. Staude, and H. Thies, Nucl. Phys. A **192**, 433 (1972).

[29] J. H. Carver, D. C. Peaslee, and R. B. Taylor, Phys. Rev. **127**, 2198 (1962).

[30] T. Deague, E. Muirhead, and B. Spicer, Nucl. Phys. A **139**, 501 (1969).

[31] N. Stone, At. Data Nucl. Data Tables **90**, 75 (2005).

[32] N. Nica, Nucl. Data Sheets **176**, 1 (2021).

[33] C. M. Baglin, Nucl. Data Sheets **111**, 275 (2010).

[34] J. Batchelder, A. Hurst, and M. Basunia, Nucl. Data Sheets **183**, 1 (2022).

[35] E. McCutchan, Nucl. Data Sheets **126**, 151 (2015).

[36] ENSDF database as of July 3, 2023, version available at http://www.nndc.bnl.gov/ensarchivals/.

[37] A. Koning, S. Hilaire, and M. Duijvestijn, in *Proceedings of the International Conference on Nuclear Data for Science and Technology - ND2007, May 22–27, 2007*, edited by O. Bersillon, F. Gunsing, E. Bauge, R. Jacqmin, and S. Leray (EDP Science, Nice, 2008), pp. 211–214.

[38] A. Koning, D. Rochman, J.-C. Sublet, N. Dzysiuk, M. Fleming, and S. van der Marck, Nucl. Data Sheets **155**, 1 (2019).

[39] B. S. Ishkhanov and V. N. Orlin, Phys. At. Nucl. **78**, 557 (2015).

[40] A. G. Kazakov, S. S. Belyshev, T. Y. Ekatova, V. V. Khankin, A. A. Kuznetsov, and R. A. Aliev, J. Radiol. Nucl. Chem. **317**, 1469 (2018).

[41] S. Agostinelli, J. Allison, K. Amako, J. Apostolakis *et al.*, Nucl. Instrum. Meth. Phys. Res., Sect. A **506**, 250 (2003).

[42] T. Tamae, T. Hino, H. Kawahara, M. Nomura, M. Sugawara, A. Tanaka, T. Tanaka, H. Tsubota, T. Yokokawa, and T. Yoshida, Nucl. Phys. A **690**, 355 (2001).

[43] K. Shoda, Phys. Rep. **53**, 341 (1979).

[44] S. Belyshev, A. Kuznetsov, and K. Stopani, EPJ Web Conf. **146**, 01011 (2017).

[45] S. S. Belyshev, D. M. Filipescu, I. Gheoghe, B. S. Ishkhanov, V. V. Khankin, A. S. Kurilik, A. A. Kuznetsov, V. N. Orlin, N. N. Peskov, K. A. Stopani, O. Tesileanu, and V. V. Varlamov, Eur. Phys. J. A **51**, 67 (2015).

[46] V. V. Varlamov, B. S. Ishkhanov, V. N. Orlin, and K. A. Stopani, Eur. Phys. J. A **50**, 114 (2014).

[47] P. Morse and H. Feshbach, *Methods of Theoretical Physics*, International series in pure and applied physics (McGraw-Hill, New York, 1953).